

## $^{15}\text{N}$ – $^1\text{H}$ Bond Length Determination in Natural Abundance by Inverse Detection in Fast-MAS Solid-State NMR Spectroscopy

Ingo Schnell<sup>†</sup> and Kay Saalwächter<sup>\*,‡</sup>

Max-Planck-Institut für Polymerforschung, Postfach 3148, D-55021 Mainz, Germany, and Institut für Makromolekulare Chemie, Universität Freiburg, Stefan-Meier-Strasse 31, D-79104 Freiburg, Germany

Received April 24, 2002

Sensitivity enhancement by  $^1\text{H}$  inverse detection<sup>1</sup> is at the present time almost universally employed in heteronuclear multidimensional NMR experiments for structure determination in solutions. For solids, it was only recently demonstrated that the  $^1\text{H}$  resolution enhancement achievable by fast magic-angle spinning (MAS) suffices to overcome the main limitation for inverse detection in the solid state, namely the broad  $^1\text{H}$  lines.<sup>2</sup> Substantial gains in sensitivity were reported for a variety of  $^{15}\text{N}$  and  $^{13}\text{C}$  systems.<sup>2–4</sup> Specific pulse sequences and detection schemes providing high  $^1\text{H}$  resolution allowed for large sensitivity gains also in inverse-detected static  $^2\text{H}$  and  $^{15}\text{N}$  powder spectra.<sup>5,6</sup> Inverse detection schemes bear particular challenges when low isotope concentrations are to be observed, because the incomplete removal of a large overhead of uncoupled  $^1\text{H}$  magnetization may lead to severe spectral artifacts. In solution-state approaches, pulsed field gradients (PFGs) have emerged as the standard procedure to destroy unwanted coherences.<sup>7</sup> For solids, it was shown that radio frequency (RF) pulses exploiting strong dipole–dipole couplings may serve the same purpose without the need for specific spectrometer hardware.<sup>4</sup>

In this communication, we present two-dimensional  $^{15}\text{N}$ – $^1\text{H}$  correlation NMR experiments with  $^1\text{H}$  inverse detection under fast MAS conditions on natural-abundance  $^{15}\text{N}$  systems. PFGs or, alternatively, RF pulses ensure suppression of unwanted  $^1\text{H}$  signal, and the acquisition of 2D spectra becomes feasible within experiment times of a few hours. It is shown for the first time that heteronuclear  $^1\text{H}$ – $^{15}\text{N}$  dipole–dipole couplings, thus bond lengths, can be faithfully extracted in natural abundance using spinning sideband patterns generated by a recently developed recoupling technique.<sup>8</sup> The large significance of high-precision bond length determination in solid-state NMR with respect to the characterization of hydrogen bonds has recently been highlighted.<sup>9</sup> In our  $^{15}\text{N}$ – $^1\text{H}$  spectra, information on (i) chemical shifts and (ii) dipole–dipole couplings/bond lengths can be accessed either individually or in a combined way using a split- $t_1$  approach.

The approach is based on the combination of two solid-state NMR techniques providing incoherent and subsequently coherent transfer of polarization between  $^1\text{H}$  and  $^{15}\text{N}$  (see Figure 1). Initial  $^1\text{H}$  polarization is incoherently transferred to  $^{15}\text{N}$  by a conventional cross-polarization (CP) step. At this point, to prepare for the final (inverse) detection of the weak  $^{15}\text{N}$  signal on  $^1\text{H}$ , strong remaining  $^1\text{H}$  polarization is efficiently removed by either a field gradient pulse (of 100  $\mu\text{s}$  duration) or by two RF pulses (of 400  $\mu\text{s}$  duration and fulfilling a rotary resonance recoupling condition),<sup>4</sup> while the  $^{15}\text{N}$  polarization is stored in a longitudinal state. Both dephasing techniques were found to perform almost identically. Aided by this preselection, the desired coherence transfer pathway

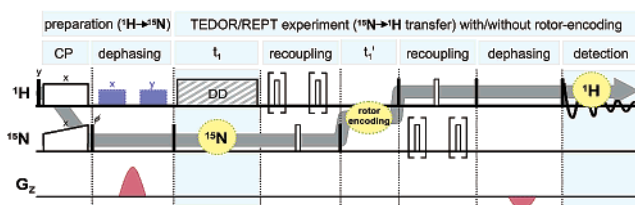


**Figure 1.** Pulse sequence for  $^1\text{H}$ -detected  $^{15}\text{N}$ – $^1\text{H}$  correlation NMR spectroscopy under fast MAS in the solid state. Solid and open bars represent  $90^\circ$  and  $180^\circ$  pulses, respectively. Alternative ways to suppress surplus  $^1\text{H}$  magnetization are shown in red (PFGs) and blue (dephasing RF pulses).

(i.e.,  $^1\text{H} \rightarrow ^{15}\text{N} \rightarrow ^1\text{H}$ ) can be selected by a four-step phase cycle and, including a final cleanup of the signal, by an overall phase cycle of 16 or 32 steps. While dephasing RF pulses are readily available on standard NMR hardware, PFGs require the installation of gradient coils at the bottom and the top of the MAS stator. Finally, the  $^{15}\text{N}$  signal is transferred back to  $^1\text{H}$  for detection using a coherent TEDOR-type<sup>8,10</sup> recoupling procedure, which allows the quantification of the  $^{15}\text{N}$ – $^1\text{H}$  coupling.

Two independent spectral dimensions can be inserted into this CP-TEDOR double-transfer scheme: a dipolar-decoupled (DD)  $^{15}\text{N}$  dimension ( $t_1$ ) between the two transfer blocks, and a  $t_1'$  dimension in the middle of the TEDOR sequence. While the former generates  $^{15}\text{N}$  chemical-shift information, the latter comprises a modulation of a dipolar-ordered state by the recoupling. This “rotor-encoding” approach has been established in other homonuclear<sup>11</sup> and heteronuclear<sup>8</sup> correlation experiments. The information on the couplings can be retrieved from the  $t_1'$ -modulation of the detected signal, which is converted into a sideband pattern by Fourier transformation. These patterns sensitively depend on the product of recoupling time and dipolar coupling constant.<sup>8</sup>

Figure 2a shows a  $^{15}\text{N}$ – $^1\text{H}$  correlation NMR spectrum of L-histidine·HCl·H<sub>2</sub>O obtained in a 2.5-mm rotor system at 30 kHz MAS. The sacrifice of signal associated with the use of small rotors, which, when applied in natural abundance, limits the technique to smaller molecules, is unfortunately unavoidable, since fast MAS is essential for an efficient and quantifiable TEDOR transfer.<sup>8</sup> However, only 8192 transients of the pulse sequence depicted in Figure 1 were needed to acquire the full 2D spectrum. To obtain a pure chemical-shift correlation spectrum,  $t_1$  was incremented in steps of full rotor periods ( $\tau_R$ ), while rotor-encoding was omitted ( $t_1' = 0$ ). In this way, natural-abundance  $^{15}\text{N}$ – $^1\text{H}$  correlation spectra can be recorded within 4–10 h and thus become routinely applicable for solids. The comparison of inverse-detected CP-TEDOR and the analogous  $^{15}\text{N}$ -detected, regular 2D TEDOR experiment yielded a sensitivity gain<sup>2</sup> of about 6–8, as detailed in the Supporting Information.

In the spectrum shown in Figure 2a, all three expected NH correlation signals are observed when the  $^{15}\text{N}$ – $^1\text{H}$  interactions are recoupled for a duration of  $2 \times 6\tau_R$  in the TEDOR step. For shorter

\* To whom correspondence should be addressed. E-mail: kays@makro.uni-freiburg.de.

<sup>†</sup> Max-Planck-Institut für Polymerforschung.

<sup>‡</sup> Institut für Makromolekulare Chemie, Universität Freiburg.

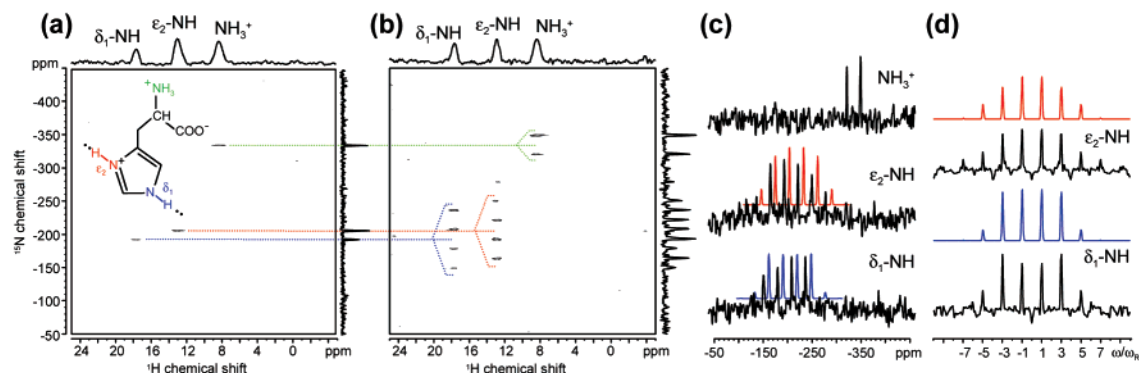


**Figure 2.** (a)  $^{15}\text{N}$ – $^1\text{H}$  correlation spectrum of L-histidine·HCl·H<sub>2</sub>O, measured at 30 kHz MAS in a 16.4 T magnet (700 MHz  $^1\text{H}$  Larmor frequency) using a recoupling time of  $2 \times 6\tau_{\text{R}}$  and accumulating the signal of 8192 transients of the pulse sequence depicted in Figure 1 (with RF dephasing and  $t_1' = 0$ ). (b) Same as in (a), but with PFG dephasing and dipolar spinning sideband patterns in the  $^{15}\text{N}$  dimension, obtained by incrementing  $t_1$  and  $t_1'$  simultaneously in steps of  $\tau_{\text{R}}$  and  $\tau_{\text{R}}/30$ , respectively. (c) Slices from (b) taken along the  $^{15}\text{N}$  dimension at the respective  $^1\text{H}$  positions. (d) Pure rotor-encoded sideband patterns obtained by incrementing only  $t_1'$ , while keeping  $t_1 = 0$  (using RF dephasing). Calculated patterns are displayed in color above the experimental ones. The N–H dipole–dipole couplings and N–H distances determined from the patterns are given in Table 1.

**Table 1.** N–H Dipole–Dipole Couplings ( $D_{\text{NH}}$ ) and Distances ( $r_{\text{NH}}$ ) Measured from the NMR Sideband Patterns Shown in Figure 2 c,d

$^1\text{H}$ signal		this work		NMR	diffraction
		$D_{\text{NH}}/2\pi$ [kHz]	$r_{\text{NH}}$ [pm]	$r_{\text{NH}}$ [pm]	$r_{\text{NH}}$ [pm]
~13 ppm ( $\epsilon_2$ )	(c)	$9.4 \pm 0.9$	$109 \pm 4$	$105 \pm 5$	$102.6 \pm 0.4$
	(d)	$9.9 \pm 0.5$	$107 \pm 2$		
~18 ppm ( $\delta_1$ )	(c)	$8.2 \pm 0.9$	$114 \pm 4$	$109 \pm 5$	$107.0 \pm 0.4$
	(d)	$8.85 \pm 0.5$	$111 \pm 2$		

<sup>a</sup> Data from previous solid-state NMR and neutron diffraction studies of L-histidine·HCl·H<sub>2</sub>O are given for comparison.<sup>9,12</sup>

recoupling times ( $< 2 \times 4\tau_{\text{R}}$ ) the signal from the rapidly rotating  $\text{NH}_3^+$  group is suppressed due to its weaker couplings. A precise quantification of the couplings is possible from spinning sideband patterns, which are introduced into the spectra by incrementing  $t_1'$  in steps of  $\tau_{\text{R}}/N$  simultaneously with  $t_1$  (split- $t_1$  approach). The integer number  $N$  determines the separation of the (odd-order only) sidebands in the spectra according to  $\Delta\nu = 2\nu_{\text{R}}/N$ , where  $\nu_{\text{R}}$  is the MAS frequency; the spectrum shown in Figure 2b was obtained with  $N = 30$ . In the TEDOR step, dipolar recoupling was again applied for  $2 \times 6\tau_{\text{R}}$ . From the resulting sideband patterns (Figure 2c),  $^{15}\text{N}$ – $^1\text{H}$  couplings can be estimated in the range of  $D_{\text{NH}}/2\pi > 2$  kHz, corresponding to N–H distances of up to 180 pm. Since the signal is distributed over a pattern in the split- $t_1$  experiment, it requires 5 to 10 times more signal accumulations than the pure chemical-shift correlation experiment.

When the  $^{15}\text{N}$  chemical-shift information is not required, the  $t_1$  dimension can be skipped, and a purely rotor-encoded signal is recorded in the  $t_1'$  dimension. Figure 2d shows the sideband patterns observed for  $\delta_1$ -NH and  $\epsilon_2$ -NH at ~18 ppm and ~13 ppm in the  $^1\text{H}$  spectrum, respectively. For signal acquisition, 20480 transients (2.5 times more than for the spectrum in Figure 2a) were used in total. The N–H distances extracted from these patterns reproduce well the results from previous investigations,<sup>9,12</sup> as can be inferred from Table 1. Apart from the usual overestimation of distances in NMR,<sup>9</sup> a further systematic error is always expected from the influence of couplings of the  $^{15}\text{N}$  to further protons. Nonetheless, distances can reliably be extracted even when the perturbing coupling is as strong as ~30% of the dominant coupling.<sup>8</sup> Note that in a system with multiple protons coupled to a single  $^{15}\text{N}$  nucleus, the technique only provides access to the dominant coupling. Two or more couplings of similar magnitude lead to destructive interference during recoupling and signal loss.<sup>8,13</sup>

In conclusion, we envision a wide applicability of this and related<sup>4,6</sup>  $^1\text{H}$  inverse detection techniques, which provide dipolar-coupling and chemical-shift information in systems with  $^{15}\text{N}$  in

natural abundance or in low isotopic concentration. In particular, the technique is valuable for investigations of N–H···N and N–H···O hydrogen bonds. With respect to biomolecules, the gain in  $^{15}\text{N}$  sensitivity, combined with the information on  $^{15}\text{N}$ – $^1\text{H}$  dipolar couplings, may help to improve NMR experiments for structure determination of peptide backbones in the solid state. Further technical development, in particular the optimization of the  $^1\text{H}$  RF circuit for detection, are expected to enhance the possible gain in signal sensitivity further and to promote the significance of  $^1\text{H}$ -detected solid-state NMR experiments.

**Acknowledgment.** We thank Manfred Hehn (Mainz) for installing the gradient coils in a commercial 2.5-mm MAS probehead, and Professors Spiess (Mainz) and Finkelmann (Freiburg) for general support. Financial aid by the DFG (SFB 428, Freiburg), the BMBF (BMBF No. 03N 6500, Mainz), and the Fonds der Chemischen Industrie is acknowledged.

**Supporting Information Available:** Further experimental details, data on the sensitivity gain, and discussion of the error limits (PDF). This material is available free of charge via the Internet at <http://pubs.acs.org>.

## References

- (1) (a) Müller, L. *J. Am. Chem. Soc.* **1979**, *101*, 4481–4484. (b) G. Bodenhausen, G.; Ruben, D. *J. Chem. Phys. Lett.* **1980**, *69*, 185–189. (c) Bax, A.; Griffey, R. R.; Hawkins, B. L. *J. Magn. Reson.* **1983**, *55*, 301–315.
- (2) (a) Ishii, Y.; Tycko, R. *J. Magn. Reson.* **2000**, *142*, 199–204. (b) Schnell, I.; Langer, B.; Söntjens, S. H. M.; van Genderen, M. H. P.; Sijbesma, R. P.; Spiess, H. W. *J. Magn. Reson.* **2001**, *150*, 57–70.
- (3) Goward, G. R.; Schnell, I.; Brown, S. P.; Spiess, H. W.; Kim, H.-D.; Ishida, H. *Magn. Reson. Chem.* **2001**, *39*, S5–S17.
- (4) Ishii, Y.; Yesinowski, J. P.; Tycko, R. *J. Am. Chem. Soc.* **2001**, *123*, 2921–2922.
- (5) Schmidt-Rohr, K.; Saalwächter, K.; Liu, S.-F.; Hong, M. *J. Am. Chem. Soc.* **2001**, *123*, 7168–7169.
- (6) Hong, M.; Yamaguchi, S. *J. Magn. Reson.* **2001**, *150*, 43–48.
- (7) Sattler, M.; Schleucher, J.; Griesinger, C. *Prog. NMR Spectrosc.* **1999**, *34*, 93–158.
- (8) Saalwächter, K.; Graf, R.; Spiess, H. W. *J. Magn. Reson.* **2001**, *148*, 398–418.
- (9) Zhao, X.; Sudmeier, J. L.; Bachovchin, W. W.; Levitt, M. H. *J. Am. Chem. Soc.* **2001**, *123*, 11097–11098.
- (10) (a) Morris, G. A.; Freeman, R. *J. Am. Chem. Soc.* **1979**, *101*, 760–761. (b) Hing, A. W.; Vega, S.; Schaefer, J. *J. Magn. Reson.* **1992**, *96*, 205–209.
- (11) (a) Graf, R.; Demco, D. E.; Gottwald, J.; Hafner, S.; Spiess, H. W. *J. Chem. Phys.* **1996**, *106*, 885–895. (b) Brown, S. P.; Schnell, I.; Brand, J. D.; Müllen, K.; Spiess, H. W. *J. Am. Chem. Soc.* **1999**, *121*, 6712. (c) Brown, S. P.; Zhu, X. X.; Saalwächter, K.; Spiess, H. W. *J. Am. Chem. Soc.* **2001**, *123*, 4275–4285. (d) Schnell, I.; Spiess, H. W. *J. Magn. Reson.* **2001**, *151*, 153.
- (12) Fuess, H.; Hohlwein, D.; Mason, S. A. *Acta Crystallogr.* **1977**, *B33*, 654–659.
- (13) Fyfe, C. A.; Lewis, A. R. *J. Phys. Chem. B* **2000**, *104*, 48–55.

JA026657X